Dynamic Kinesthetic Boundary for Haptic Teleoperation of Aerial Robotic Vehicles

Xiaolei Hou and Robert Mahony

Abstract— This paper introduces a novel dynamic kinesthetic boundary to aid a pilot to navigate an aerial robotic vehicle through a cluttered environment. Classical haptic teleoperation interfaces for aerial vehicles utilize force feedback to provide the pilot with a haptic feel of the robot's interaction with an environment. The proposed approach constructs a dynamic kinesthetic boundary on the master device that provides the pilot with hard boundaries in the haptic workspace to indicate approaching obstacles. An advantage of the proposed approach is that when the vehicle is flying free of obstacles, then the haptic feedback of the joystick can be used to provide a more natural feel of the vehicle dynamics. Furthermore, rather than a gradual onset of virtual potential forces that are felt in the classical approaches, a pilot encountering the dynamic kinesthetic boundary is immediately aware of the presence of the obstacle and can act accordingly. The approach is implemented on an admittance haptic joystick to ensure that the haptic boundaries are faithfully rendered. We prove that in the case of perfect velocity tracking, the proposed algorithm will ensure the vehicle never colliding with the environment. Experiments were conducted on a robotic platform and the results provide verification of the novel approach.

I. INTRODUCTION

Bilateral force feedback or haptic teleoperation has its origin dating back to mid 1940s and still remains an active research topic even after 60 years development. The early work [6], [13] on bilateral force feedback teleoperation system for robotic manipulator inspired the research on haptic teleoperation of mobile robots, which has drawn significant attention in recent years [8], [14], [7], [3], [15], [5]. The standard approach models the mobile robot as a simple mass point and teleoperates the robot by coupling the dynamic states of the mass with joystick under impedance framework. Due to the mismatch of the master and slave workspace, a direct coupling using a spring-damper system between the haptic joystick and the robot restricts the workspace that the slave can reach. The classical solution to this problem is to couple the joystick position to the robot's velocity and achieves unlimited workspace [3], [12], [14], [8].

In addition to perception of the dynamics of the robot, collision avoidance for mobile robots is also required for a human operator to pilot a vehicle moving through a cluttered environment, especially for aerial robotic vehicles due to their highly dynamic nature. Force feedback has demonstrated superior performance in mobile robot teleoperation comparing to the no feedback approaches in [15], [1] for the navigation of mobile robot in the environment with scattered obstacles. The papers [10], [11], [12], [1] provided comprehensive comparisons among various schemes for obstacle avoidance in haptic control of helicopters. In [16] and [20], optic flow is used to render force feedback for flying robot obstacle avoidance. In recent work, experimental comparisons of obstacle avoidance algorithms are performed by Brandt [2]. It is noticeable that the optic flow approach in [16] and [20] is mathematically expressed with a velocity over distance form as similar as the time-to-contact approach in [2] and the *Generalized Potential Field* and the *Parametric Potential Field* approaches in [1]. All of these works lead to a similar conclusion that the obstacle avoidance approaches based on velocity over distance generally provides better performance for the pilot in haptic teleoperation of aerial robots.

Force feedback is considered as the sole haptic cue for pilot to perceive the surrounding environment and the dynamics of the vehicle in all the above works. Horan *et al* [7] presented a new interface for haptic control of a mobile robot by constructing a haptic control surface on the master device. The position of the contact point on the surface is mapped to the angular and linear velocity reference to the robot controller. Work by Hou [8] proposed admittance control for haptic teleoperation of mobile robots to enhance the pilot's perception of the vehicle's dynamic motion. The force applied by the pilot is measured and mapped to velocity set point for a robot's velocity controller; the velocity of the robot is mapped to the position reference input to the haptic joystick to servo. A user study demonstrated superior performance over the classical impedance control haptic interfaces. Work by Kim [9] exploited another way for rendering the scattered obstacles in the environment for robotic manipulators. A *Restriction Space Projection* (RSP) concept is introduced to provide human operator with the feel of the *Instantaneous Restriction Space* (IRS) where the manipulator can not reach either due to the obstacles or the geometric constraints by rendering the force accordingly.

In this paper, we propose a novel dynamic kinesthetic boundary (DKB) approach for obstacle avoidance in haptic teleoperation of aerial robots. The proposed approach is based on recent work by the authors that uses an admittance framework for servo control of aerial vehicles where the master position is servo controlled to match the slave vehicle's velocity. The slave vehicle is itself velocity controlled drawing its reference set point from the force applied to the master joystick. The dynamic kinesthetic boundary is derived from the vehicle's velocity and the distance from vehicle to obstacles in an analogous manner to the optic flow based

Xiaolei Hou and Robert Mahony are with Research School of Engineering, College of Engineering and Computer Science, Australian National University, Canberra 0200, Australia `xiaolei.hou, robert.mahony@anu.edu.au`

criteria [16] or Brandt's work [2] established in the literature. It is possible, and indeed common for the continuous evolution of the servo position associated with the vehicle state to move outside of the constraint set by the DKB. In this case we compute the *God object* [21] on the boundary and servo the master to its position, rendering the impact of the master with the boundary without imposing an impact on the vehicle. The pilot can only feel the obstacle forces when the end effector of the master device encounters the virtual boundary, otherwise the master device works under normal operating mode. The velocity set point that is sent to the slave is also modified from the instant that the DKB becomes active. We provide a lemma that proves that under the supervision of DKB, the vehicle can approach close to the obstacle at a designate distance, but does not collide with the environment. Experiments were carried out on a robotic platform, and the results demonstrate the performance of the dynamic haptic boundary approach.

The remainder of this paper is organized as follows. Section II describes the proposed approach and its implementation. The experimental setup and results are presented and analyzed in Section III. A discussion of the performance of the proposed approach against other approaches is provided. Section IV concludes the paper.

II. DYNAMIC KINESTHETIC BOUNDARY

In this section, we first introduce the haptic interface developed in Computer Vision and Robotics group at the Australian National University. The novel dynamic kinesthetic boundary (DKB) approach for obstacle avoidance is proposed for haptic teleoperation of aerial robots in cluttered environment, and its implementation in the haptic interface is also provided.

A. Haptic Interface

The under-actuated attitude dynamics of the flying robot are controlled by a high gain closed loop attitude controller [17], [18]. Therefore the robot can be modeled as a simplified second order system,

$$
\begin{aligned}
\dot{x} &= v \\
m\dot{v} &= f
\end{aligned}
\tag{1}
$$

where $x \in \mathbb{R}^3$, $v \in \mathbb{R}^3$ and $f \in \mathbb{R}^3$ are the position of the vehicle, the velocity and the force applied to vehicle respectively.

There are two types of haptic interfaces that are typically used by researchers in haptic teleoperation, admittance interface and impedance interface. Under the admittance interface, the causality of the haptic interface in Fig. 1 is inverse to the impedance interface in Fig. 2. The haptic joystick measures the force input from user and converts this force into the velocity set point for the vehicle's velocity controller, and servos the position reference mapped from velocity feedback of the robot.

$$
\begin{aligned}
\dot{x}_{\text{ref}} &= k_1 f_{\text{user}} \\
\xi_{\text{ref}} &= k_2 \dot{x}
\end{aligned}
\tag{2}
$$
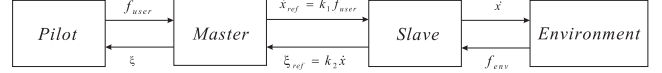
Fig. 1. System structure of the admittance haptic interface
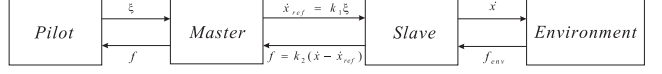
Fig. 2. System structure of the impedance haptic interface

where k_1 is the scaling factor from user force input f to velocity set point $\dot{x}_{\text{ref}} \in \mathbb{R}^3$, and k_2 is the scaling factor from robot's velocity $\dot{x} \in \mathbb{R}^3$ to joystick's position $\xi_{\text{ref}} \in \mathbb{R}^3$. Whereas the impedance interface takes the position measurement of the joystick as the velocity reference input for the robot to servo, and feeds back the force to the pilot according to the velocity information of the vehicle,

$$
\begin{aligned}
\dot{x}_{\text{ref}} &= k_1\xi \\
f &= k_2(\dot{x} - \dot{x}_{\text{ref}})
\end{aligned}
\tag{3}
$$

where k_1 is the scaling factor from user position input ξ to velocity set point $\dot{x}$, and k_2 is the gain for generating force feedback f.

According to the outcomes of our previous research [19], [8], the admittance interface has demonstrated superior performance over the classical impedance interface in haptic teleoperation of mobile robots. In addition, the admittance haptic modalities will allow direct implementation of the proposed DKB, whereas an impedance interface would require an algorithm to stably render contact forces [4], [21].

B. Dynamic Kinesthetic Boundary

The dynamic kinesthetic boundary (DKB) that we propose is a virtual hard boundary implemented in the master joystick's workspace. It is constructed based on the distance information to the obstacles. Velocity constraints are applied accordingly to achieve obstacle avoidance.

Consider spherical coordinates in the body fixed frame (BFF) of the vehicle represented by radial distance λ, azimuth θ and elevation ϕ. Let $\eta(\theta, \phi) \in S^2$ denote the unit directional vector associated with angle pair (θ, ϕ). That is

$$
\eta(\theta, \phi) = \begin{pmatrix} \cos(\theta)\cos(\phi) \\ \sin(\theta)\cos(\phi) \\ \sin(\phi) \end{pmatrix} \in S^2.
\tag{4}
$$

Let $\lambda(\theta, \phi, t) \in \mathbb{R}$ denote the radial distance from the body-fixed frame of the mobile vehicle to the first obstacle along bearing direction $\eta(\theta, \phi)$ at time t. The maximum speed of the vehicle is denoted $v_{\max} \geq 0$. We use two parameters, the safety distance d_{sf} and the threshold distance d_{th} to encode thresholds that limit how close the vehicle will approach obstacles. The dynamic kinesthetic boundary (DKB) $\beta(\theta, \phi, t)$ is defined by

$$
\beta(\theta, \phi, t) = \min\{k_2 \frac{\lambda(\theta, \phi, t) - d_{\text{sf}}}{d_{\text{th}}} v_{\max}, k_2 v_{\max}\}
\tag{5}
$$

where k_2 is the scaling factor from robot's velocity to joystick's position.
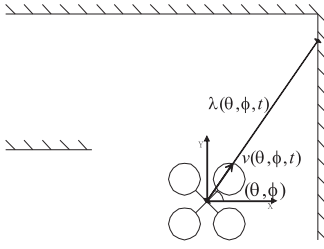
Fig. 3.   Example

Fig. 4.   Example DKB

Fig. 5.   DKB implementation in admittance framework for perceiving obstacle avoidance
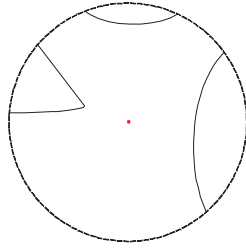
The safety distance d_{sf} should include the radius of the robot, and the threshold distance d_{th} should be tuned according to the requirement of the task. The closer to the obstacles the task requires, the smaller d_{sf} should be tuned; the bigger d_{th} is, the earlier the DKB will be encountered.

The DKB is implemented by setting the master joystick to servo to reference position $\xi_{\text{ref}}(t)$ by

$$\xi_{\text{ref}}(t) = \begin{cases} k_2 v(t), & \text{if } k_2\|v(t)\| \leq \beta(\theta_v, \phi_v, t) \\ \\ \beta(\theta_v, \phi_v, t)\eta(\theta_v, \phi_v), & \text{if } k_2\|v(t)\| > \beta(\theta_v, \phi_v, t) \end{cases}$$

$$(6)$$

where (θ_v, ϕ_v) is the bearing of the velocity $v(t)$ of vehicle in BFF. That is $v = \|v\|\eta(\theta_v, \phi_v)$. Note that (θ_v, ϕ_v) is not uniquely defined for $\|v\| = 0$. This does not affect the proposed algorithm in any way and we will arbitrarily choose $(\theta_v, \phi_v) = (0, 0)$ in this case.

When the end-effector of the joystick has no contact with the DKB, the user does not feel the DKB and the haptic interface operates under normal working mode. Otherwise the pilot will perceive the DKB and the haptic joystick's workspace is bounded by the DKB.

An example of the real world scenario with DKB on the joystick is shown in Fig. 3 and 4. According to (5), the DKB varies as the robot approaches or departs from obstacles, and has its maximum range of $k_2 v_{\max}$ when the obstacles are not in the sight or further than $d_{\text{th}} + d_{\text{sf}}$ away from the robot, and the minimum value of zero when obstacles approach to the safety distance d_{sf}. Note that planar obstacle maps to curved coordinates due to d_{th} and d_{sf} in (5).

C. Obstacle Avoidance

In addition to providing the pilot with a feel for obstacles in the environment, the DKB provides an ideal mechanism to implement obstacle avoidance for the vehicle. We propose that velocity reference to the robot's controller is scaled with respect to the DKB,

$$v_{\text{ref}}(t) = \begin{cases} k_1 f_{\text{user}}(t), & \text{if } k_1\|f_{\text{user}}(t)\| \leq \frac{\beta(\theta_f, \phi_f, t)}{k_2} \\ \\ \frac{\beta(\theta_f, \phi_f, t)}{k_2}\eta(\theta_f, \phi_f), & \text{if } k_1\|f_{\text{user}}(t)\| > \frac{\beta(\theta_f, \phi_f, t)}{k_2} \end{cases}$$

$$(7)$$

where k_1 is the scaling factor from user force input to velocity set point, and (θ_f, ϕ_f) denotes the bearing of the user force input f_{user}. That is $f_{\text{user}} = \|f_{\text{user}}\|\eta(\theta_f, \phi_f)$.

Similar to the boundary implementation, the scaling of velocity references only becomes effective when the reference input meets the boundary condition; Otherwise it remains ineffective.
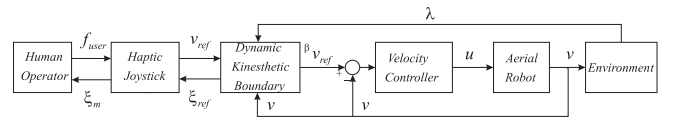
The system architecture for the proposed dynamic kinesthetic boundary on an admittance haptic joystick is shown in Fig. 5. The DKB provides obstacle avoidance and is perceived by the user as follows: the sensor data is collected and used to construct the DKB according to (5), the force input from user is measured and fed into the DKB module for scaling according to (7), the scaled velocity set points are sent to velocity controller of the slave robot, and the admittance joystick is controlled to servo the position reference mapped from the velocity of the vehicle using (6).

D. Analysis

Lemma 2.1: Assume that the vehicle is flying in a locally smooth environment with bounded curvature. Given the proposed scheme and assuming exact velocity tracking $v = v_{\text{ref}}$ of the vehicle, $\forall t > 0$

$$\lambda(\theta, \phi, t) - d_{\text{sf}} > 0. \qquad (8)$$

Proof:
Define

$$y(t) = \min_{(\theta, \phi) \in S^2} (\lambda(\theta, \phi, t) - d_{\text{sf}}). \qquad (9)$$

Let (θ^*, ϕ^*) denote azimuth-elevation pair that realizes $y(t) = \lambda(\theta^*, \phi^*, t) - d_{\text{sf}}$. Such an (θ^*, ϕ^*) always exists since S^2 is compact.

The proof proceeds by contradiction.

Assume there exists a first finite time $t_0 > 0$, such that

$$\lim_{t \to t_0} y(t) = 0. \qquad (10)$$

Hence $\forall t < t_0$, $y(t) > 0$. Since the environment is assumed to be locally smooth with bounded curvature, there must exist $t_1 < t_0$, such that for all $t_1 < t < t_0$, (θ^*, ϕ^*) is continuously differentiable and hence $y(t)$ is also differentiable.

According to (7) and since we assume $v = v_{\text{ref}}$, the actual velocity is always bounded by the DKB velocity

$$\frac{\lambda(\theta, \phi, t) - d_{\text{sf}}}{d_{\text{th}}} v_{\max} \geq \langle v(t), \eta(\theta, \phi) \rangle \geq -\|v(t)\| \qquad (11)$$

and in particular this is true for $(\theta, \phi) = (\theta^*, \phi^*)$. From (11) and recalling definition of $y(t)$ in (9), then for $t \in [t_1, t_0]$, one has

$$y(t) = \frac{d_{\text{th}}}{v_{\max}} \langle v(t), \eta(\theta^*, \phi^*) \rangle. \qquad (12)$$

Differentiating $y(t)$ yields

$$\frac{d}{dt} y(t) = \frac{\partial\lambda(\theta^*, \phi^*, t)}{\partial\theta^*}\dot{\theta}^* + \frac{\partial\lambda(\theta^*, \phi^*, t)}{\partial\phi^*}\dot{\phi}^* + \frac{\partial\lambda(\theta^*, \phi^*, t)}{\partial t}.$$

$$(13)$$

Note that $\frac{\partial\lambda(\theta^*, \phi^*, t)}{\partial\theta^*}\dot{\theta}^* = 0$ and $\frac{\partial\lambda(\theta^*, \phi^*, t)}{\partial\phi^*}\dot{\phi}^* = 0$ since (θ^*, ϕ^*) is the minimizer of (9) and the environment is
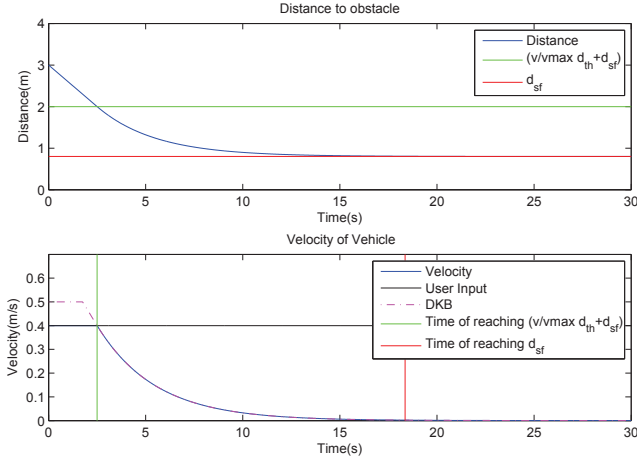
Fig. 6. Simulation result of a constant velocity reference input of $0.4m/s$, (Parameters: $v_{\text{max}} = 0.5$, $d_{\text{th}} = 1.5$, $d_{\text{sf}} = 0.8$, $\lambda(0) = 3$)
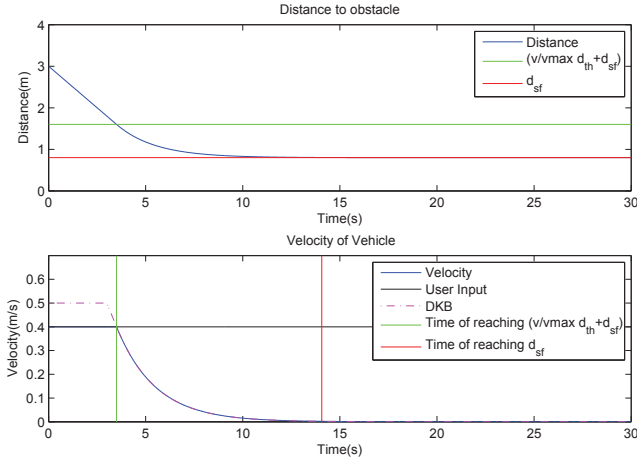
Fig. 7. Simulation result of a constant velocity reference input of $0.4m/s$, (Parameters: $v_{\text{max}} = 0.5$, $d_{\text{th}} = 1$, $d_{\text{sf}} = 0.8$, $\lambda(0) = 3$)

locally smooth. It is straight to verify that $\frac{\partial \lambda(\theta^*, \phi^*, t)}{\partial t} = -\langle v(t), \eta(\theta^*, \phi^*) \rangle$, equation (13) thus becomes

$$\frac{d}{dt} y(t) = -\langle v(t), \eta(\theta^*, \phi^*) \rangle = -\frac{v_{\text{max}}}{d_{\text{th}}} y(t). \qquad (14)$$

Therefore on the time interval $t_1 < t < t_0$, one has

$$\dot{y}(t) = -\frac{v_{\text{max}}}{d_{\text{th}}} y(t), \qquad y(t_1) > 0 \qquad (15)$$

and hence $y(t) = e^{-(t-t_1)\frac{v_{\text{max}}}{d_{\text{th}}}} y(t_1)$ and $\lim_{t \to t_0} y(t) \neq 0$ contradicting the assumption (10). It follows that there is no first finite time t_0 such that $y(t) \to 0$, and since $(\lambda(\theta, \phi, t) - d_{\text{sf}}) \geq y(t)$, the result is proved. ■

E. Simulation

A simple simulation was performed where the vehicle approached a flat wall with constant input from user.

In Fig. 6, the vehicle started at 3 meters away from the obstacle and traveled towards the obstacle with constant reference input of $0.4m/s$ from the user. As the vehicle approached the obstacle, the DKB was encountered from approx. $2.5s$ and started to limit the velocity of the vehicle.
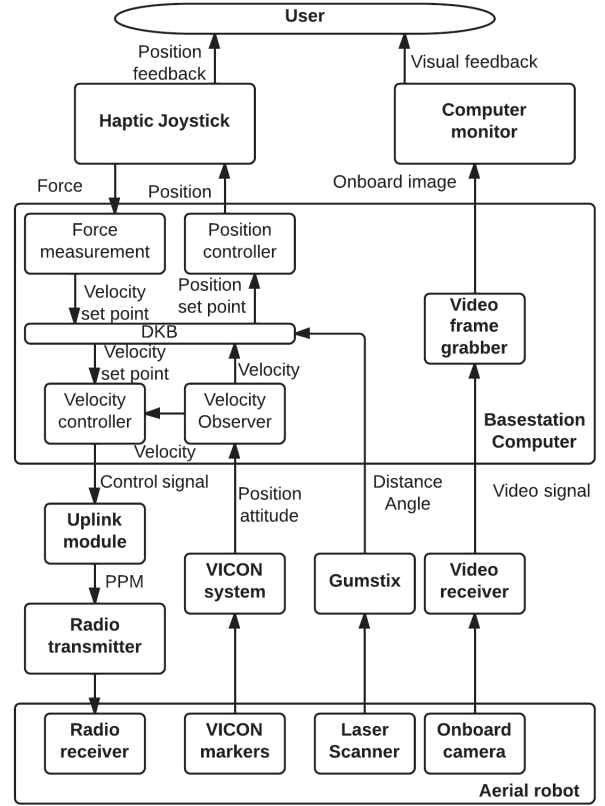
Fig. 8. Implementation of robotic platform and haptic interface

Eventually the vehicle came to rest at the safety distance d_{sf} indicated by the red line. This result shows that the DKB can effectively regulate the velocity of the vehicle and prevents the vehicle from colliding with the environment.

In Fig. 7, simulation was repeated with the same parameters as previous test except $d_{\text{th}} = 1$. Due to the smaller threshold distance d_{th}, the DKB was encountered later (approx. $3.5s$) than that in previous simulation, but the vehicle reached the safety distance and stopped earlier (approx. $14.2s$) at the safety distance d_{sf} indicated by the red line. The outcomes of simulation indicate that, the behavior of the vehicle can be regulated according to the tasks requirements, i.e. fast or slow approach near obstacles, by tuning the threshold distance d_{th}.

III. EXPERIMENT

This section presents the physical implementation of the proposed dynamic kinesthetic boundary on an experimental robotic platform and the experimental setup for verifying the effectiveness of the DKB approach. The results from experiments are then provided for analysis.

A. Experiment facility

The DKB approach is implemented on an admittance haptic joystick for controlling an experimental robotic platform shown in Fig. 8. The experimental haptic teleopration system consists of the following components.
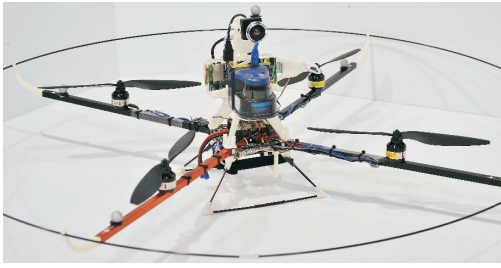
Fig. 9.   Aerial robot
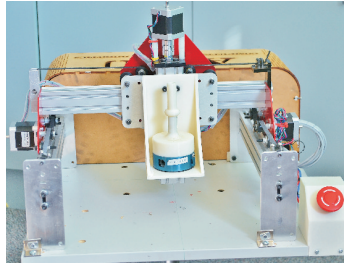
Fig. 10.   Admittance haptic joystick
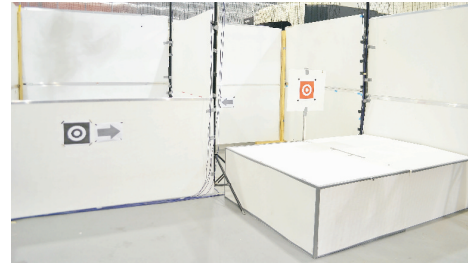
Fig. 11.   Experimental environment

a) Haptic joystick: A customized made 3DoF admittance haptic joystick was developed as shown in Fig. 10. A JR3 force sensor is equipped to measure the force and torque inputs from the pilot to control three translational motions and one rotational motion. This admittance joystick is running at 1KHz with a USB interface.

b) Aerial robot: A Mikrokopter quadrotor, shown in Fig. 9, is used as the flying platform to carry all the necessary equipments for performing the tasks, including a hokuyo laser scanner, an ultrasonic sensor, a gumstix computer and an onboard camera. The hokuyo laser scanner provides the distance data of up to 4 meters range with 270 degrees field of view at 35Hz, which is mounted on top of the quadrotor facing the front. Due to the limited field of view of the laser scanner, to monitor the obstacles behind the vehicle, an ultrasonic sensor is integrated into the system pointing backward. An ARM based gumstix computer running ROS (Robot Operating System) collects all the sensor data and transmits it back to the base station through WIFI connection for rendering the DKB. An onboard camera with a 5.8GHz transmitter is equipped to provide the pilot with a real time 110 degrees field of view visual feedback.

c) VICON visual tracking system: The VICON visual tracking system provides real time information of vehicle's position and attitude at 200Hz to facilitate to estimate and regulate the velocities of the robot.

d) Experimental environment: A cluttered environment is constructed under the supervision of the VICON visual tracking system in Fig. 11. The dimension of this environment is of $1.8 \ meters \ \times 4.8 \ meters \ \times 4.8 \ meters$.

B. Experimental scenarios

Two experimental scenarios are designed to verify the applicability and effectiveness of the proposed DKB approach.

1) Scenario A: The first scenario is designed to verify the obstacle avoidance behavior directly. The pilot hovers near a flat wall and then repeatedly attempts to fly into the wall. The expected behavior is that as the distance from the robot to the flat wall decreases below $d_{\text{th}} + d_{\text{sf}}$, the DKB will slow the vehicle's velocity by limiting the maximum velocity reference input. The vehicle will never approach closer than the safety distance d_{sf}.

2) Scenario B: In this scenario, the user will pilot the vehicle along a predefined course through a complex structure. The pilot needs to fly through a series of narrow corridors and avoid the internal walls and the obstacles in the environment.
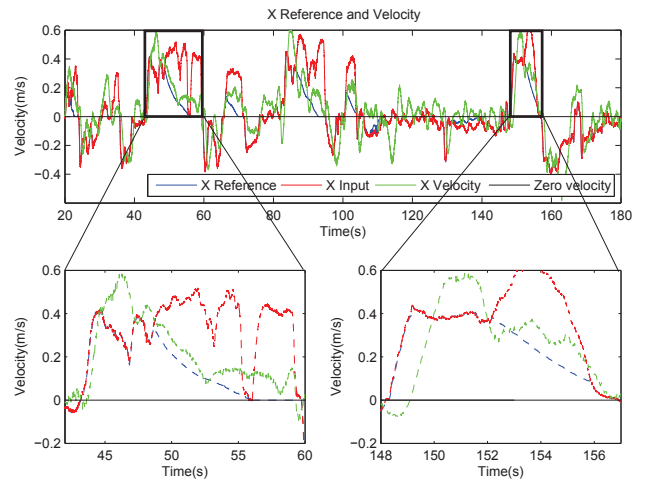
Fig. 12.   Scenario A (single axis response, zoomed-in figures show attempts to collide with obstacles)

It is expected that the DKB will both ensure no collisions occur, and additionally provide the user with a natural feel for the vehicle's interaction with the environment.

C. Experimental Results

Two sets of data of two scenarios are collected from experiments and shown in Fig. 12 and Fig. 13. The user input, the actual reference sent to the robot and the robot's velocity are illustrated by the red, blue and green dashed lines respectively.

Fig. 12 shows the experimental data of scenario A. Note the similar trend of the velocity signals when the DKB is active as was seen in Simulations Fig. 6 and 7. This is particularly clear in the zoomed data in Fig. 12.

The data of the flight through the experimental environment is shown Fig. 13. The primary motion of the vehicle during the trajectory was in the x- and y- axis and not in the z- axis and hence we plot only these two axes to visualize the data. There were no collisions during flight despite several points where the DKB was active. The zoomed data shows one point in the flight where the DKB was active and prevented a collision. The pilot found that the feel of the haptic response was natural and provided an intuitive feel for the environment interaction.

D. Discussion

The *Lemma*, simulation and experimental results all provide evidence that the dynamic kinesthetic boundary can

Fig. 13. Scenario B (flight through obstacle strewn environment, zoomed-in figures show close approach to obstacles)

effectively prevent the vehicle from colliding with the obstacles and help a pilot safely navigate through a complex environment.

Different from the conventional force feedback approach, the DKB approach we propose exploits a new methodology to achieve effective obstacle avoidance in haptic teleoperation of mobile robots. We believe the DKB has its advantages in obstacle avoidance for the navigation of mobile robot for the following reasons:

1) Distinguishable haptic cue from the force feedback: standard bilateral force feedback teleoperation systems only provide force feedback to the pilot to perceive both the dynamics of the robot and the obstacle avoidance force [3], [12], [16], [1]. The mixed force may cause the pilot's confusions about the situation and lead to possible collisions. The DKB approach employs a completely different haptic cue to indicate the obstacles in the environment. We thus believe the DKB approach can better warn pilot of potential collisions than force feedback.

2) Guaranteed performance for obstacle avoidance: Lemma 2.1 provides a proof that the vehicle can never collide into obstacles. The simulation and experimental results also agree with this same conclusion. By contrast, many force feedback based obstacle avoidance algorithms [2], [16] give no such guarantee.

IV. CONCLUSIONS

In this paper, we propose a novel approach for obstacle avoidance and haptic teleoperation of aerial robots based on a novel concept of dynamic kinesthetic boundary. This approach exploits a new methodology of providing obstacle avoidance in haptic teleoperation of mobile robots. Simulation and experimental results presented support the claims of the analysis and verify the effectiveness of the proposed approach.

REFERENCES

[1] H. W. Boschloo, T. M. Lam, M. Mulder, and M. M. van Paassen. Collision avoidance for a remotely-operated helicopter using haptic feedback. In *Proc. 2004 IEEE Int. Conf. Syst. Man Cybern.*, volume 1, pages 229 –235 vol.1, 0-0 2004.

[2] A. M. Brandt and M. B. Colton. Haptic collision avoidance for a remotely operated quadrotor uav in indoor environments. In *Proc. 2010 IEEE Int. Conf. Syst. Man Cybern.*, pages 2724 –2731, oct. 2010.

[3] N. Diolaiti and C. Melchiorri. Teleoperation of a mobile robot through haptic feedback. In *Proc. 2002 IEEE Int. Workshop Haptic Virtual Environments and Their Applications*, pages 67 – 72, 2002.

[4] N. Diolaiti, G. Niemeyer, F. Barbagli, and J. K. Salisbury. Stability of haptic rendering: Discretization, quantization, time delay, and coulomb effects. *IEEE Trans. on Robot.*, 22(2):256–268, 2006.

[5] I. Elhajj, N. Xi, W. K. Fung, Y. H. Liu, W. J. Li, T. Kaga, and T. Fukuda. Haptic information in internet-based teleoperation. *Trans. Mechatron.*, 6(3):295 –304, sep 2001.

[6] B. Hannaford. A design framework for teleoperators with kinesthetic feedback. *IEEE Trans. on Robot. and Autom.*, 5(4):426 –434, aug 1989.

[7] B. Horan and S. Nahavandi. Intuitive haptic control surface for mobile robot motion control. In *Proc. 2008 IEEE Int. Workshop Safety, Security and Rescue Robot.*, pages 121 –127, oct. 2008.

[8] X. Hou, R. Mahony, and F. Schill. Representation of vehicle dynamics in haptic teleoperation of aerial robots. In *Proc. 2013 IEEE Int. Conf. Robot. and Autom.*, pages 1447–1483, may 2013.

[9] K. Kim, W. K. Chung, and I. H. Suh. Accurate force reflection for kinematically dissimilar bilateral teleoperation systems using instantaneous restriction space. In *Proc. 2006 IEEE Int. Conf. Robot. and Autom.*, pages 3257 –3262, may 2006.

[10] T. M. Lam, M. Mulder, and M. M. van Paassen. Haptic feedback for uav tele-operation - force offset and spring load modification. In *Proc. 2006 IEEE Int. Conf. Syst. Man Cybern.*, volume 2, pages 1618 –1623, oct. 2006.

[11] T. M. Lam, M. Mulder, and M. M. van Paassen. Collision avoidance in uav tele-operation with time delay. In *Proc. 2007 IEEE Int. Conf. Syst. Man Cybern.*, pages 997 –1002, oct. 2007.

[12] T. M. Lam, M. Mulder, and M. M. van Paassen. Haptic interface in uav tele-operation using force-stiffness feedback. In *Proc. 2009 IEEE Int. Conf. Syst. Man Cybern.*, pages 835 –840, oct. 2009.

[13] D. A. Lawrence. Stability and transparency in bilateral teleoperation. *IEEE Trans. on Robot. and Autom.*, 9(5):624 –637, oct 1993.

[14] D. Lee and K. Huang. Passive-set-position-modulation framework for interactive robotic systems. *IEEE Trans. on Robot.*, 26(2):354 –369, april 2010.

[15] S. Lee, G. S. Sukhatme, G. J. Kim, and C. M. Park. Haptic control of a mobile robot: a user study. In *Proc. 2002 IEEE/RSJ Int. Conf. Intell. Robots Syst.*, volume 3, pages 2867 – 2874, 2002.

[16] R. Mahony, F. Schill, P. Corke, and Y. S. Oh. A new framework for force feedback teleoperation of robotic vehicles based on optical flow. In *Proc. 2009 IEEE Int. Conf. Robot. and Autom.*, pages 1079 –1085, may 2009.

[17] D. Mellinger, N. Michael, and V. Kumar. Trajectory generation and control for precise aggressive maneuvers with quadrotors. *Int. J. Robot. Res.*, 31(5):664–674, 2012.

[18] P. Pounds, R. Mahony, and P. Corke. Modelling and control of a large quadrotor robot. *Control Engineering Practice*, 18(7):691–699, 2010.

[19] F. Schill, X. Hou, and R. Mahony. Admittance mode framework for haptic teleoperation of hovering vehicles with unlimited workspace. In *Proc. 2010 Australian Conf. Robot. Autom.*, Dec 2010.

[20] F. Schill, R. Mahony, P. Corke, and L. Cole. Virtual force feedback teleoperation of the insectbot using optical flow. In *Proc. 2008 Australasian Conf. Robot. Autom.*, Canberra, Australia, dec. 2008.

[21] C. B. Zilles and J. K. Salisbury. A constraint-based god-object method for haptic display. In *Proc. 1995 IEEE/RSJ Int. Conf. Intell. Robots Syst.*, volume 3, pages 146 –151 vol.3, aug 1995.